

## Chapter 11

# Biomimetic Approaches to Gas Phase Peptide Chemistry: Combining Selective Binding Motifs with Reactive Carbene Precursors to Form Molecular Mousetraps

Accepted for publication in: Julian, R. R.; May, J. A.; Stoltz, B. M.; Beauchamp, J. L.  
*Int. J. Mass Spectrom.*

### 11.1 Introduction

In the post genomic world of proteomics,<sup>1</sup> many substantial advances will be made through experiments conducted in the gas phase. Therefore, understanding and (ultimately) controlling gas phase peptide chemistry is of paramount importance. For example, the study of gas phase peptide chemistry has revealed that selective cleavage of the peptide backbone will occur at aspartic acid residues.<sup>2,3</sup> It has been further demonstrated that this cleavage occurs by a displacement reaction that yields a stable five-membered ring. Understanding this phenomenon allows for the accurate prediction of peptide cleavages in aspartic acid containing peptides. Furthermore, C-terminal peptide sequencing via a similar mechanism where the C-terminal amino acids are sequentially removed has also yielded promising, if limited, results.<sup>4</sup> Unfortunately, this C-terminal sequencing is restricted to peptides with 8 amino acids or less, severely

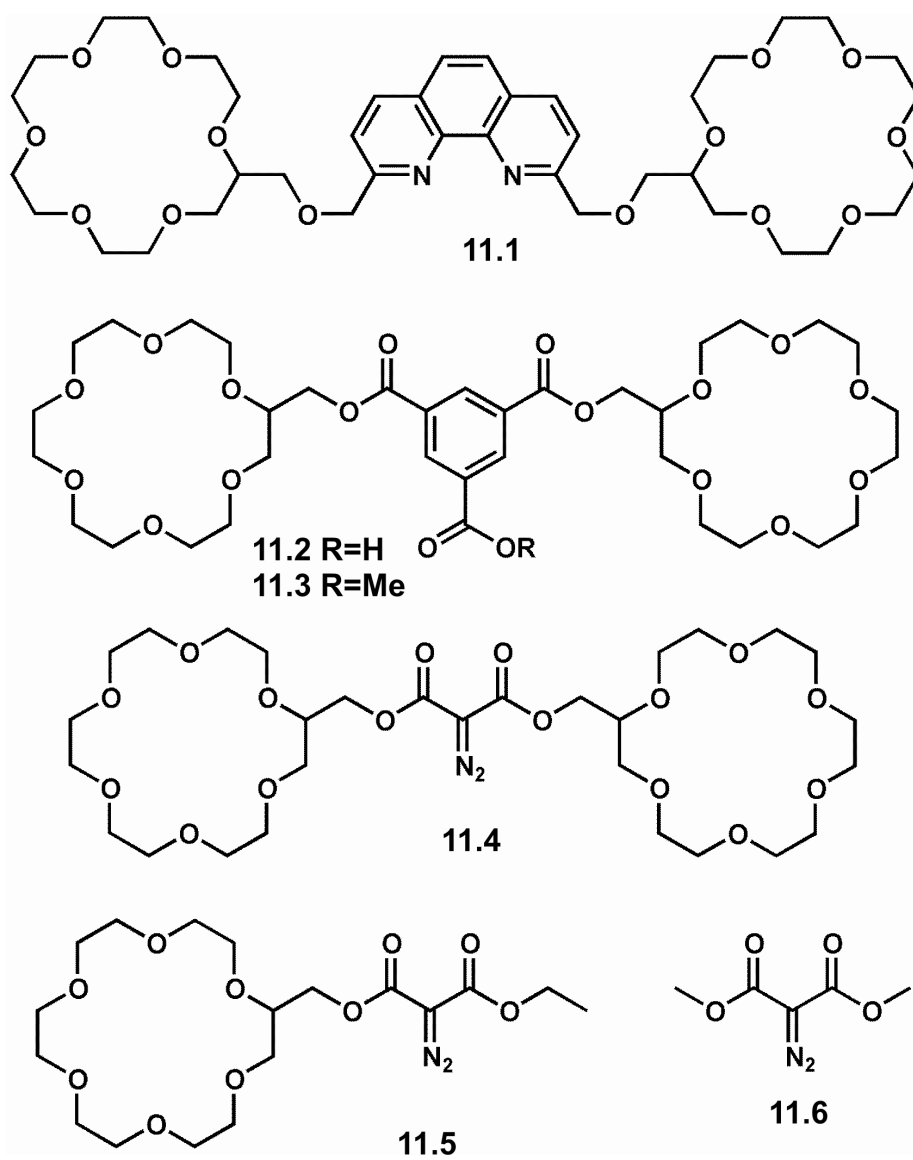
curtailing the ability of this technique to sequence proteins in the gas phase. The addition of transition metals can also mediate peptide chemistry in the gas phase.<sup>5,6</sup> Preliminary studies have shown that Zn<sup>2+</sup>, Ni<sup>2+</sup>, and Co<sup>2+</sup> will attach to histidine and promote peptide fragmentation at this residue.<sup>5</sup> These experiments were carried out on a very limited sampling of peptides, but the resulting cleavages were highly specific. Similarly, Fe<sup>2+</sup> complexes with cysteine containing peptides enhanced the number of cleavages observed at the cysteine residues when the peptide was collisionally activated. These important initial results illustrate that peptide chemistry can be influenced by the addition of appropriate reagents.

In an effort to develop experimental methodologies for the controlled manipulation of peptides in the gas phase, we have undertaken a systematic study to develop *de novo* reagents capable of selectively attaching to and reacting with peptides in the gas phase. It is envisioned that these reagents will be capable of initiating a wide range of chemical reactions, such as peptide backbone cleavage at specific residues, as described above. With appropriate modifications, the type of reagents proposed herein could serve as fluorescent probes, chemical cross-linkers, and sequence specific binding agents. In the present work we consider two reagents (**11.1** and **11.2**) designed to initiate selective cleavage of the peptide backbone near lysine residues. In addition, we present reagents **11.4** and **11.5** designed to covalently attach to lysine containing peptides following appropriate activation which generates a reactive carbene center. We first discuss considerations that led to the design of these reagents.

Reagents **11.1-11.5** all rely on molecular recognition of specific amino acid side chains to form specific noncovalent complexes in the gas phase. Fortunately, a significant amount of work developing reagents that selectively recognize and noncovalently attach

to specific amino acid side chains has already been reported.<sup>7,8,9</sup> These side chain hosts represent the first and simplest form of a biomimetic reagent, one that is only capable of recognition. It should be noted that the facile formation of noncovalent complexes is critical to the success of this type of experiment, and proper conditions for enhancing noncovalent complex formation have been studied extensively.<sup>10,11</sup>

**Chart 11.1**



18-crown-6 ether (18C6) was chosen as the recognition and binding motif because it is both synthetically flexible and amenable to noncovalent complexation. It is well known for its ability to bind both metal cations and protonated primary amines in both solution and in the gas phase.<sup>12</sup> This ability is particularly useful for the recognition of lysine, because the side chain of this amino acid terminates in a primary amine. 18C6 complexes protonated primary amines through a combination of three hydrogen bonds and ion-dipole interactions. Noncovalent complexes with 18C6 bound to protonated primary amines can be transferred into the gas phase by electrospray ionization mass spectrometry (ESI-MS). When added to a solution containing a peptide, the 18C6 complex with the peptide is typically the most abundant peak in the spectrum.<sup>8</sup> Appropriately modified lariat crown ethers behave similarly, forming noncovalent complexes that can be transferred to the gas phase as shown previously<sup>13</sup> and in the present work.

Lariat crown ethers **11.1** and **11.2** were synthesized and tested to determine their ability to selectively cleave various peptides. While these reagents did not demonstrate optimal reactivity, yielding limited results with regards to peptide cleavage, they serve to illustrate the important factors in biomimetic reagent design. Greater success was achieved with reagents **11.4** and **11.5**, which are designed to covalently attach to peptides. These two reagents containing diazo groups were complexed with a series of small molecules and peptides. Collisional activation was utilized to generate a carbene from the diazo functionality without dissociation of the complex. The intermolecular reactions were studied with ESI-MS and density functional theory (DFT). Sequential MS<sup>n</sup> spectra revealed covalent bond attachment between the constituents of the complex subsequent to the generation of the carbene. The data demonstrate that the insertion

reactions are sensitive to the presence or absence of N-H and O-H functional groups. The present work expands upon our previous work reporting initial experiments with this class of reagents that we have termed molecular mousetraps.<sup>14</sup>

## 10.2 Experimental

**Mass Spectrometry.** All spectra were obtained using a Finnigan LCQ ion trap quadrupole mass spectrometer without modification. The critical instrument settings that yield adduct formation include capillary voltage 5-15V, capillary temperature 200°C, and tube lens offset -30 to -50V. Higher capillary temperatures can dissociate the noncovalent complexes. The tube lens offset controls the acceleration of ions as they leave the capillary region. The tube lens voltage is minimized to avoid collisions with the He buffer gas. Soft sampling is crucial for the detection of these noncovalent complexes.

Sample concentrations were typically kept in the ~10 to 100  $\mu\text{M}$  range for all species of interest. All samples were electrosprayed in a mixture of 80:20 methanol/water. The appropriate host was added to the sample and electrosprayed with the guest in order to observe adducts. Collision activated dissociation (CAD) was performed by isolating and then exciting the isolated peak by colliding it with He buffer gas. Samples were electrosprayed with a flow of 3-5  $\mu\text{L}/\text{min}$  from a 500  $\mu\text{L}$  Hamilton syringe for optimal signal. Silica tubing with an inner diameter of .005 in was used as the electrospray tip.

**Calculations.** The energetics of the carbene insertion reactions were quantitatively evaluated by carrying out reactions with the model compound **11.6**. The structures of all reactants were fully minimized, and several different reaction mechanisms were tested. Initial structures included likely starting points for hydrogen abstraction, concerted

insertion, and ylide formation. The starting structures for each of these possibilities corresponded respectively to: one hydrogen directed at the carbene, symmetrical presentation of the H-C-H or O-H bonds, and one lone pair directed at the carbene. The DFT calculations were carried out using Jaguar 4.1 (Schrödinger, Inc., Portland, Oregon). PM5 semi-empirical calculations were carried out using CACHe Worksysterm Pro 5.04 (Fujitsu, Inc., Beaverton, Oregon).

**Experimental Details for Syntheses:** Due caution should always be used when handling diazo compounds. Reactions were performed in flame-dried glassware under a nitrogen atmosphere. Solvents were dried and purified using activated alumina columns. Diethylamine was distilled from  $\text{CaH}_2$ . 18-crown-6-methanol was dried prior to use by heating ( $\sim 100$  °C) under vacuum. All other reagents were used as received from commercial sources. Reaction temperatures were controlled by an IKAmag temperature modulator.

**Compound 11.1:** To a stirred solution of diethylamine (13  $\mu\text{L}$ , 0.123 mmol) in THF (500  $\mu\text{L}$ ) at 0 °C was added nBuLi (60  $\mu\text{l}$ , 2.1 M, 0.126 mmol) dropwise. The mixture was stirred for 10 min and then transferred via syringe to a solution of 18-crown-6-methanol (30  $\mu\text{L}$ , 0.109 mmol) in THF (500  $\mu\text{L}$ ) stirred at -78 °C. The solvent was removed under reduced pressure as the reaction warmed to room temperature. Excess diethylamine was removed by two consecutive additions of THF (1 mL) and removal under reduced pressure. The residue was then redissolved in THF (1 mL) and 2,9-bis(bromomethyl)-1,10-phenanthroline<sup>15</sup> (19 mg, 0.052 mmol) in  $\text{CH}_2\text{Cl}_2$  (4 mL) was added. The resulting solution was stirred for 24 hours, and then ether (10 mL) was added to precipitate the salt byproduct, which was removed by filtration through celite. The

removal of solvent under reduced pressure yielded **11.1** (37.5 mg, 0.047 mmol, 91% yield) in sufficient purity for experimental use.

**Compound 11.2:** To a stirred solution of 18-crown-6-methanol (47  $\mu$ l, 0.150 mmol), triethylamine (25  $\mu$ l, 0.179 mmol), and dichloromethane (4.5 ml) was added 1,3,5-benzenetricarbonyl trichloride (20.4 mg, 0.077 mmol). The mixture was heated to reflux for 12 hours, and then  $\text{H}_2\text{O}$  (1.5 mL) was added and the mixture was again heated to reflux for 1 hour. The solvent was removed under reduced pressure, the residue dissolved in a minimal amount of dichloromethane (500  $\mu$ l), and the undesired salts were precipitated out of solution with the addition of ether (5 ml). Filtration through celite and removal of solvent under reduced pressure yielded **11.2** (54.2 mg, 0.071 mmol, 95% yield) in sufficient purity for experimental use.

**Compound 11.3:** An identical procedure as that for the formation of **11.2** was followed with the exception that the reaction was quenched with MeOH (500  $\mu$ L) instead of  $\text{H}_2\text{O}$  to yield **11.3** (49.1 mg, 0.063 mmol, 82% yield) in sufficient purity for experimental use.

**Compounds 11.4 and 11.5** were prepared according to the method described in Chapter 10.

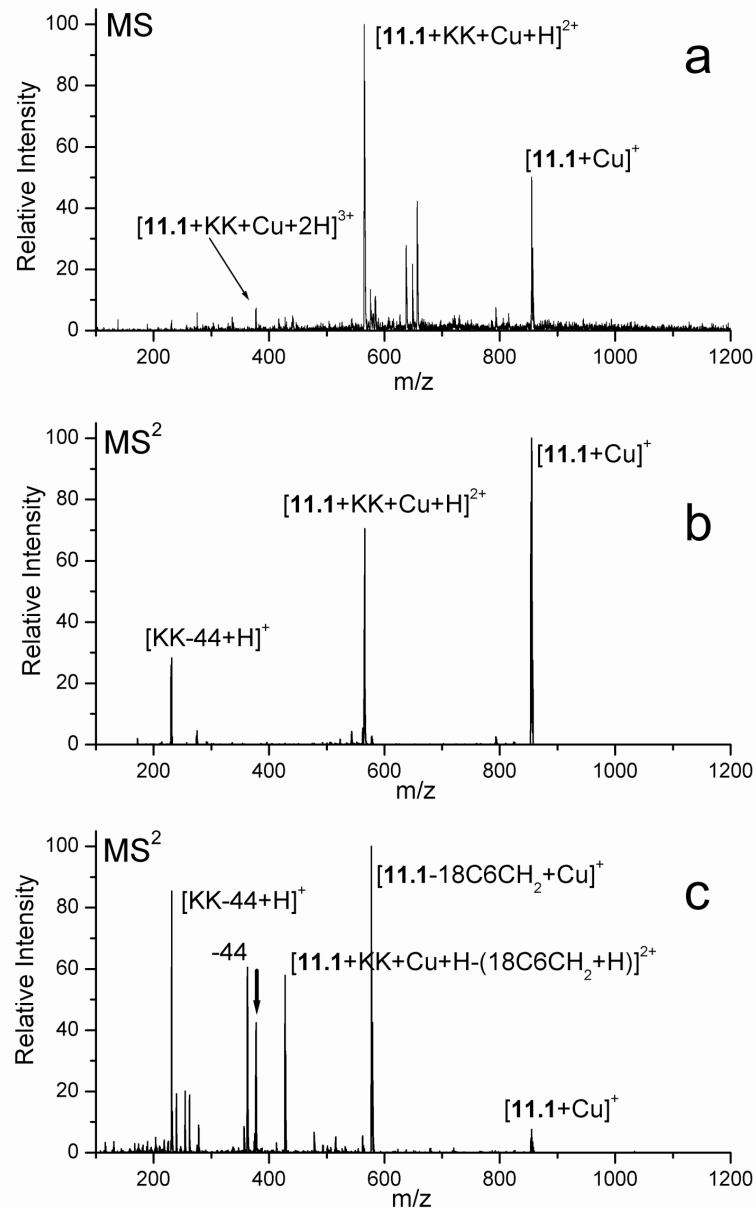
### 11.3 Results and Discussion

Transition metals have been observed to influence peptide dissociation in previous gas phase experiments.<sup>5,6</sup> In an attempt to utilize the reactivity of transition metals for the selective cleavage of peptide bonds, reagent **11.1** was developed. **11.1** consists of two 18C6 ethers linked by a phenanthroline moiety, which can bind a variety of transition metals. Figure 11.1a shows that **11.1** forms an abundant noncovalent complex with the

peptide KK and copper (I). Collisional activation of the base peak  $[11.1+KK+Cu+H]^{2+}$  results primarily in dissociation of the complex into  $[11.1+Cu]^+$  and  $[KK+H]^+$  with an additional prominent peak corresponding to the loss of 44 Da from  $[KK+H]^+$ . This loss is most likely explained as elimination of  $CO_2$  from the C-terminus. In Figure 11.1c, collisional activation of the much less abundant complex  $[11.1+KK+Cu+2H]^{3+}$  yields the loss of  $CO_2$  directly. In the absence of the copper (I) ion, no loss of 44 Da is observed for either charge state, suggesting that copper (I) effectively initiates this reaction. Unfortunately, this chemistry only occurs with very short peptides that end with KK or RK, and reagent **11.1** did not initiate any other cleavages. A wide variety of peptides and different transition metals including Ag(I), Fe(III), Co(II), Zn(I), Zn(II), Mn(II), Ni(II), Pd(II) and Cu(II) were tested. Many of these experiments failed to produce an abundant noncovalent complex, and when the complex was formed and isolated the result was simple dissociation in every case where the peptide contained an internal KK sequence.

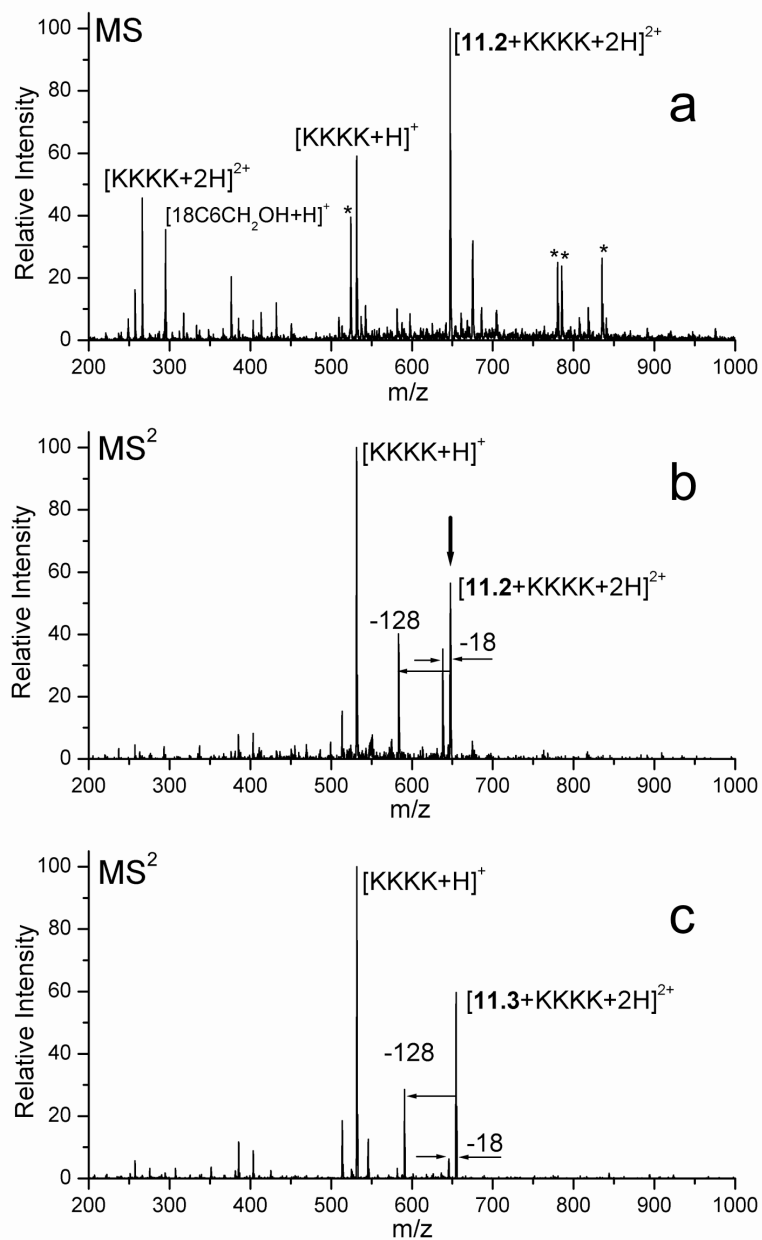
These results can be rationalized by insufficient binding energy of the noncovalent complex in the gas phase. The presence of a cationic transition metal trapped between two positively charged lysine residues results in unfavorable coulombic interactions that effectively reduce the binding energy of the complex. The binding energy is reduced by  $\sim 80 \pm 10$  kcal/mol for inserting a singly charged transition metal ion as determined by PM5 calculations. This explains why only minimal complexation (or none) occurs for internal KK sequences, and the reduced binding also leads to the exclusive dissociation of these complexes upon collisional activation. A deprotonated C-terminus effectively mitigates the unfavorable interactions and increases the binding energy by neutralizing the central positive charge. Therefore, reagent **11.1** is suitable for selectively attaching

near the C-terminus of peptides that end in KK or RK/KR, however it did not prove effective at cleaving peptides in the gas phase.



**Figure 11.1** (a) ESI-MS of 11.1, copper (I), and KK. An abundant complex is formed. (b)  $MS^2$  on the doubly charged complex results in simple dissociation. (c)  $MS^2$  on the triply charged complex results in the loss of  $CO_2$  from the C-terminus of the peptide. Bold downward arrow indicates the peak being subjected to collisional activation.

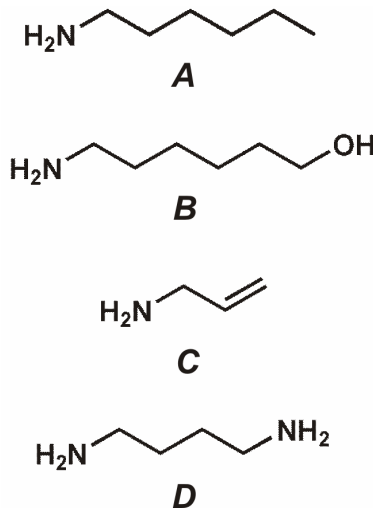
As mentioned above, selective cleavage at aspartic acid residues has been observed in the gas phase previously, indicating that acid/base chemistry may provide an alternate route for cleaving peptides in the gas phase.<sup>2,3</sup> Reagent **11.2** was designed based upon this premise. **11.2** contains two 18C6 ethers linked by benzoic acid. Deprotonation of the acid is assisted by favorable electrostatic interactions upon complexation with two protonated lysine residues. The ESI mass spectrum for a solution of **11.2** and KKKK is shown in Figure 11.2a. The doubly charged adduct  $[\mathbf{11.2}+\text{KKKK}+2\text{H}]^{2+}$  forms the base peak in the spectrum. Collisional activation of this peak results primarily in dissociation of the complex. However, there are additionally two peaks corresponding to the loss of water and the N-terminal lysine. To verify that this chemistry was initiated by the benzoic acid, an additional experiment was conducted where the acid was converted to a methyl ester (**11.3**). The results are shown in Figure 11.2c and are nearly identical to those shown in Figure 11.2b.



**Figure 11.2** (a) ESI-MS of KKKK with **11.2**, demonstrating excellent recognition. (b)  $MS^2$  on the base peak leads to the loss of the N-terminal lysine. (c) Control experiment with **11.3** yields same results as in (b), suggesting that **11.2** is merely a spectator adduct and does not initiate the cleavage of the N-terminal lysine. Bold downward arrow indicates the peak being subjected to collisional activation.

Therefore it is likely that **11.2** is merely a spectator adduct, which is sufficiently strongly bound to remain attached after a covalent bond cleavage has occurred but does not directly affect the cleavage process. Earlier studies of selective cleavages at aspartic acid residues suggest that this process is favored due to the proximity of the aspartic acid side chain to the peptide backbone, with acidity enhanced by a proximal positive charge.<sup>2</sup> The observation that the similar reactivity of glutamic acid (with the addition of a single methylene) is greatly reduced in comparison suggests that the reaction has very special geometrical constraints. It may be that the acidic group in **11.2** cannot exploit the same reaction pathway as inferred for aspartic acid cleavages because it is not held in close proximity to the peptide backbone. Nevertheless, the results from **11.2** are important because they demonstrate that biomimetic reagents with multiple crown ethers have sufficient binding energy to mitigate dissociation in favor of peptide cleavage processes.

Although the cleaving of peptide bonds remains an important goal, covalent attachment to peptides is another important reaction that is often used for cross linking peptides and proteins.<sup>16</sup> Molecular mousetraps **11.4** and **11.5** are designed to covalently attach to peptides containing lysine residues or any other molecule which contains a protonated primary amine. Both **11.4** and **11.5** contain a reactive diazo group, which yields a highly reactive carbene upon collisional activation. Experimental and theoretical results for the interactions of **11.4** with 1,6-diaminohexane have been reported previously.<sup>14</sup> In order to understand the underlying chemistry, we have performed several experiments with simple small molecules to further elucidate the reaction pathways.

**Chart 11.2**

**Reactions with Small Molecules.** In Figure 11.3a, the ESI spectrum for a solution of 1-aminohexane (**A**) and **11.4** is shown. The complex corresponding to  $[11.4+A+H]^+$  clearly forms the base peak in the spectrum, demonstrating the excellent recognition of **11.4** for protonated primary amines. This complex is subjected to collisional activation in Figure 11.3b. The loss of N<sub>2</sub> is the only major product observed, yielding the reactive carbene (denoted by :**11.4**) in nearly 100% yield. Theoretical results at the B3LYP/6-31G\*\* level with methane and the similar carbene :**11.6** suggest that C-H insertion occurs with little or no barrier in a concerted fashion.<sup>17</sup> In Figure 11.3b, the carbene (:**11.4**) can react with **A** by C-H insertion at various points along the hydrocarbon chain. This is confirmed in Figure 11.3c, where no dissociation of **A** is observed after further collisional activation. Instead several covalent bond cleavages are observed, corresponding to the loss of a CH<sub>2</sub>CH<sub>2</sub>O link from 18C6 and another corresponding to the loss of an entire crown. This suggests that C-H insertion does in fact occur and leads to the covalent attachment of the host/guest complex.

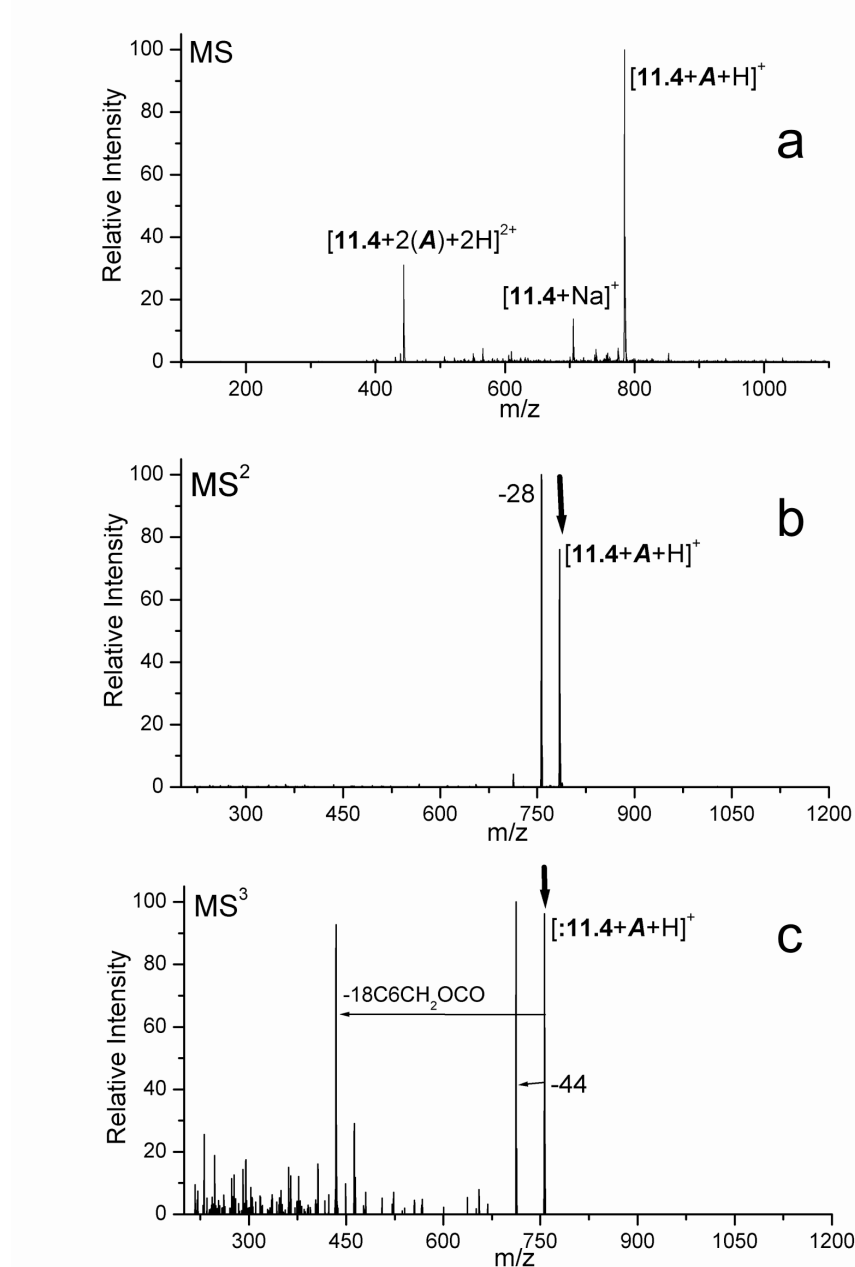


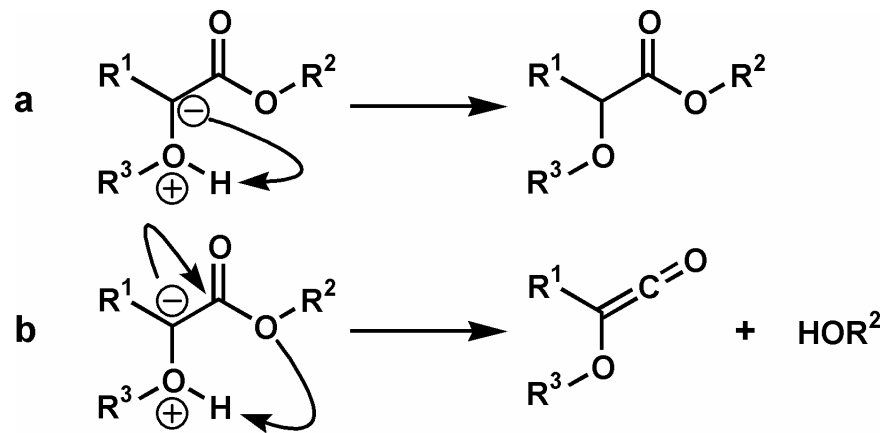
**Figure 11.3** (a) ESI-MS of 1-aminohexane (*A*) and **11.4** demonstrating excellent recognition. (b)  $MS^2$  on the base peak leads primarily to the loss of  $N_2$  and the generation of the corresponding carbene. (c) Further excitation does not result in loss of *A*, suggesting that an intermolecular insertion reaction has occurred. Bold downward arrow indicates the peak being subjected to collisional activation.

Hydroxyl groups are found in three amino acid side chains and can exhibit enhanced reactivity towards carbenes. Figures 11.4a and 11.4b show the results for CAD experiments with **11.4** and 1,6-aminohexanol (**B**) which is used as a model compound. In Figure 11.4a, the CAD of  $[\mathbf{11.4}+\mathbf{B}+\mathbf{H}]^+$  leads to similar results to those obtained previously for 1,6-diaminohexane.<sup>14</sup> The initial loss of  $\mathbf{N}_2$  is accompanied by an additional loss of  $18\mathbf{C}_6\mathbf{CH}_2\mathbf{OH}$ . The  $\mathbf{MS}^3$  spectrum is shown in Figure 11.4b for the CAD of  $[\mathbf{:11.4}+\mathbf{B}+\mathbf{H}]^+$ . The loss of  $\mathbf{CH}_2\mathbf{CH}_2\mathbf{O}$  leads to the base peak in Figure 11.4b while the loss of  $18\mathbf{C}_6\mathbf{CH}_2\mathbf{OH}$  is secondary. The loss of  $\mathbf{CH}_2\mathbf{CH}_2\mathbf{O}$  is not present in the  $\mathbf{MS}^2$  spectrum in Figure 11.4a. This suggests that the loss of  $18\mathbf{C}_6\mathbf{CH}_2\mathbf{OH}$  in Figure 11.4a and 11.4b proceed by two different reaction mechanisms and that the two products produced in Figure 11.4a are generated competitively rather than consecutively.

The two proposed reaction pathways are shown in Scheme 11.1 and are similar to those proposed for the comparable 1,6-diaminohexane system.<sup>14</sup> DFT calculations on **:11.6** and  $\mathbf{H}_2\mathbf{O}$  at the B3LYP/6-31G\*\* level support the formation of an intermediate oxonium ylide. The formation of the ylide proceeds without barrier from several different starting geometries. Precedence for this mechanism can be found in previous studies, which have revealed oxonium ylide formation in reactions of various alcohols with carboethoxycarbene, a closely related molecule.<sup>18</sup> All of the experimental and theoretical data support the reaction mechanisms shown in Scheme 11.1 for any system with an alcohol (unprotonated amines react by a very similar pathway as shown previously).<sup>14</sup> In fact, the additional loss of 294 in the  $\mathbf{MS}^2$  spectrum is indicative of the presence of alcohols and amines. In Figure 11.4c, further excitation of the complex following the loss of one  $18\mathbf{C}_6$  results primarily in the loss of the other  $18\mathbf{C}_6$  without the accompanying

loss of any **B**. In the absence of both crowns, the retention of the **B** can only be explained by an insertion reaction which has transformed the noncovalent complex into a molecule.

**Scheme 11.1**



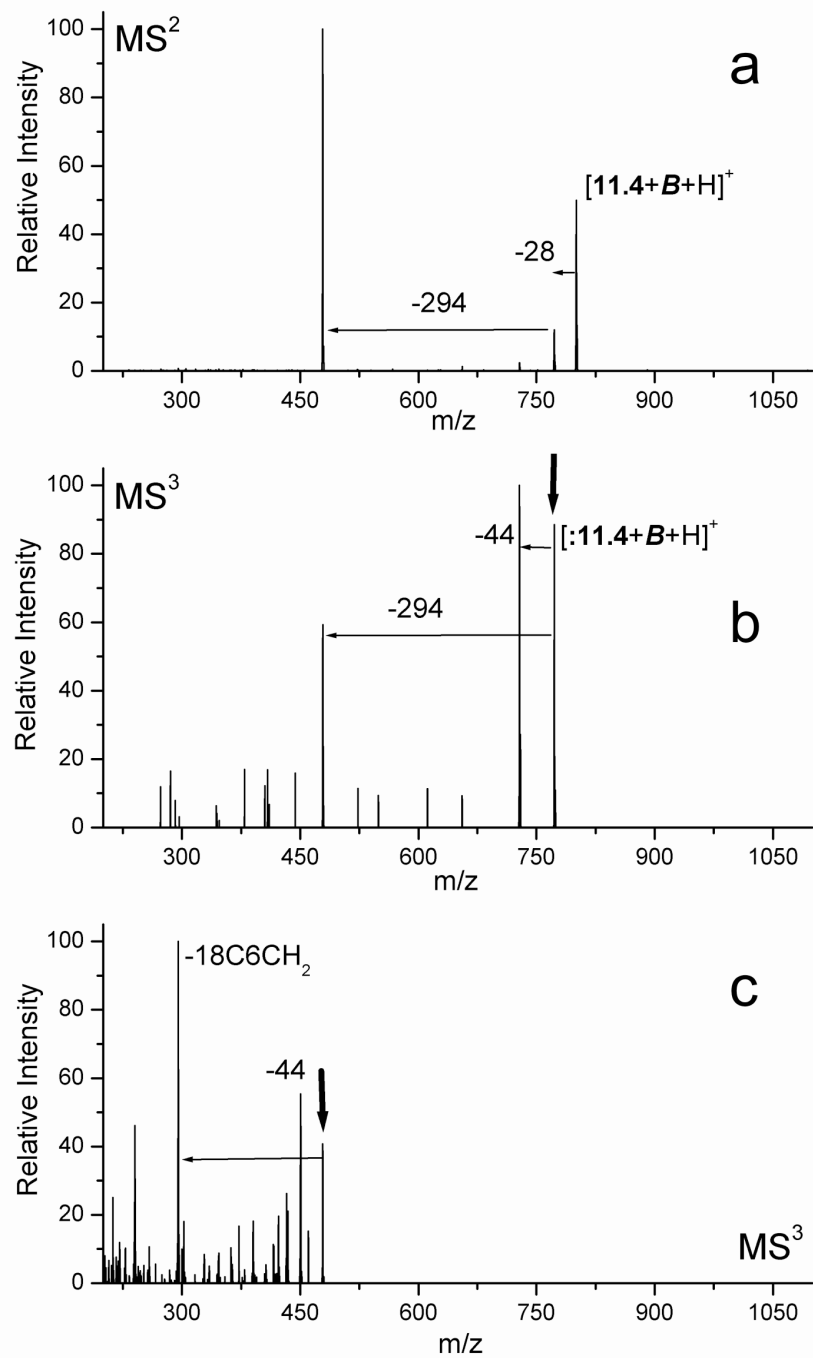


**Figure 11.4** a)  $MS^2$  on  $[4+B+H]^+$  yields similar results to those for 1,6-diaminohexane. b)  $MS^3$  spectrum is notably different, suggesting that peaks produced in (a) occur competitively. c) Further excitation of the complex does not result in any dissociation of the **B**. Bold downward arrows indicate peaks being subjected to CAD.

Reagent **11.5** contains only a single crown ether connected to a diazo functional group, with an ethyl ester connected to the side opposite 18C6. The results for complexing allylamine (**C**) and 1,4-diaminobutane (**D**) with reagent **11.5** are given in Figure 11.5. Collisional activation of the complex  $[11.5+C+H]^+$  results primarily in the loss of  $N_2$  (Figure 11.5a). Further excitation of the product peak yields the loss of neutral EtOH and a multitude of other peaks in Figure 11.5b. However, dissociation of **C** is not observed, suggesting that covalent attachment has been achieved. Carbene insertion into double bonds is a well documented phenomena in solution and is the most likely explanation for the results observed here.<sup>19</sup>

Experiments with **D** and **11.5** yield results similar to those obtained with host **11.4** and protonated 1,6-diaminohexane except that the loss of EtOH is observed in addition to the loss of  $18C6CH_2OH$ . In Figure 11.5c it is shown that the loss of EtOH is approximately twice as abundant as the loss of  $18C6CH_2OH$ . This is consistent with the proposed reaction mechanisms. In Figure 11.5d, a fragment that contains no 18C6 is subjected to CAD. **D** (mass 88 Da) does not dissociate from the complex. Since there is no crown ether present to bind to a primary amine, the data in Figure 11.5d offers compelling evidence that indeed what was once a noncovalent complex is now a molecule.

All of the data obtained by reactions with small molecules suggests that covalent attachment occurs rapidly and almost exclusively when the complex containing **11.4** or **11.5** is subjected to CAD. The corresponding carbenes (**:11.4** and **:11.5**) can undergo insertion reactions with a wide variety of different functional groups. The appropriate next step is to see whether these reagents can covalently attach to peptides themselves.

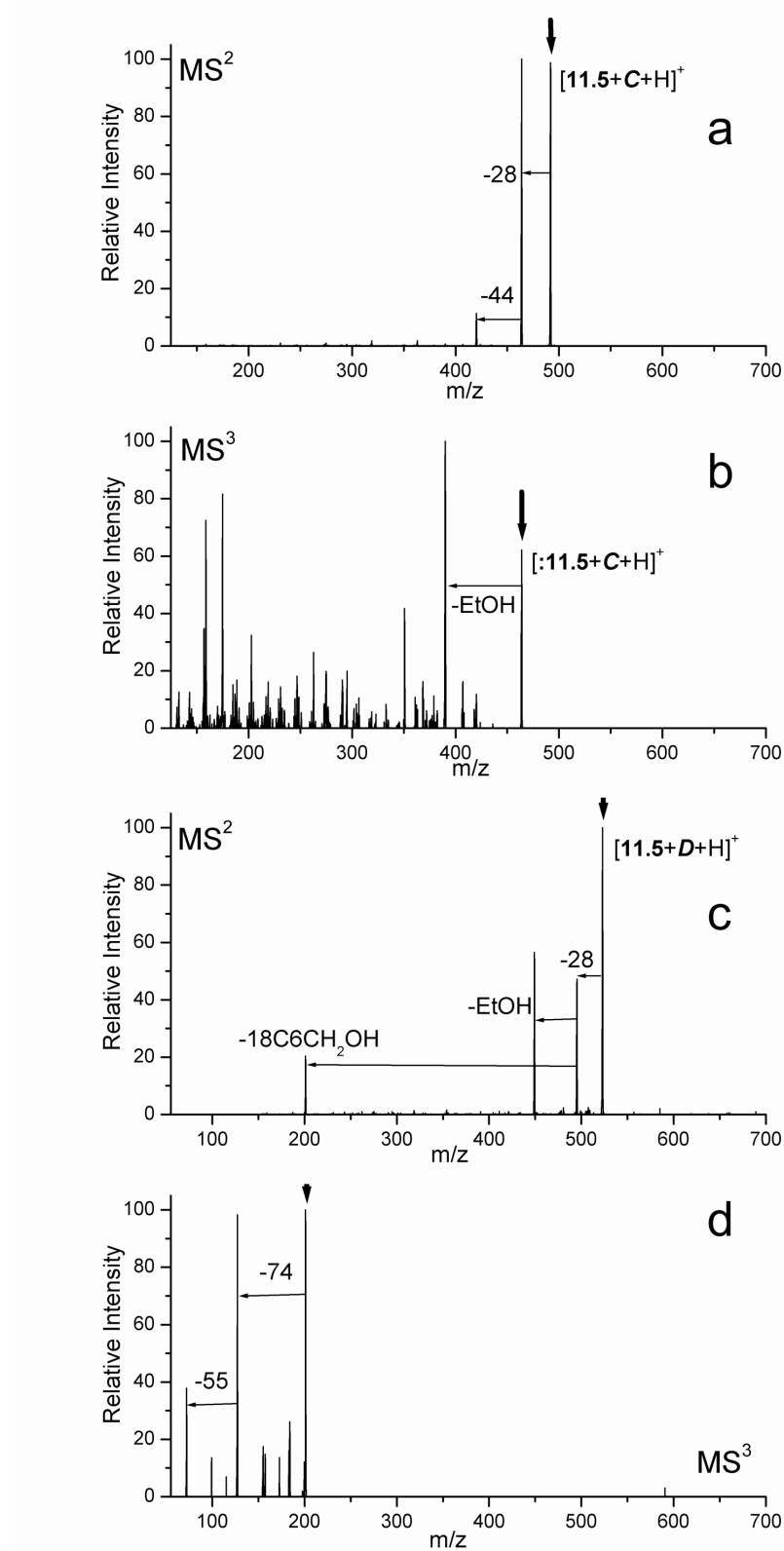


**Figure 11.5** Caption on next page.

**Figure 11.5** Experimental results for host **2**. a) MS<sup>2</sup> on complex with allylamine (**C**) results in the loss of N<sub>2</sub>. b) MS<sup>3</sup> spectrum reveals many fragmentation pathways, none of which lead to dissociation of the guest. c) CAD spectrum of 1,4-diaminobutane (**D**) and **11.2** loses N<sub>2</sub>, EtOH, and 18C6CH<sub>2</sub>OH. d) MS<sup>3</sup> spectrum on peak containing no 18C6 ring fragments rather than dissociating, offering compelling evidence for covalent attachment between the host and guest. Bold downward arrows indicate peaks being subjected to CAD.

**Peptides.** Reagent **11.4** is designed to bind to peptides containing two lysine residues. The ESI spectrum for **11.4** complexed with the simple peptide KGK is shown in Figure 11.6a. Abundant adduct peaks are observed, indicating excellent recognition. In Figure 11.6b, the  $[\mathbf{11.4}+\text{KGK}+2\text{H}]^{2+}$  peak is subjected to collisional activation. The loss of N<sub>2</sub> leads to the base peak in the spectrum, with an additional loss of 294 Da being observed as well. No dissociation is observed, suggesting that the appropriate combination of high binding energy and low activation barriers has been achieved for reagent **11.4**. Further collisional activation in Figure 11.6c does not lead to any dissociation of KGK, again confirming that an intermolecular reaction has occurred. Very similar results are obtained for other peptides containing two lysines in close proximity, such as INLKAI AALVKKVL, AAKRKAA, and KK. If the singly charged  $[\mathbf{11.4}+\text{KGK}+\text{H}]^+$  complex is subjected to CAD, then a neutral loss of **11.4** yields the only observed product. This appears to suggest that two crown ethers are necessary to achieve sufficient binding energy for the intermolecular reaction to occur. However, it will be demonstrated below that this is not the case.

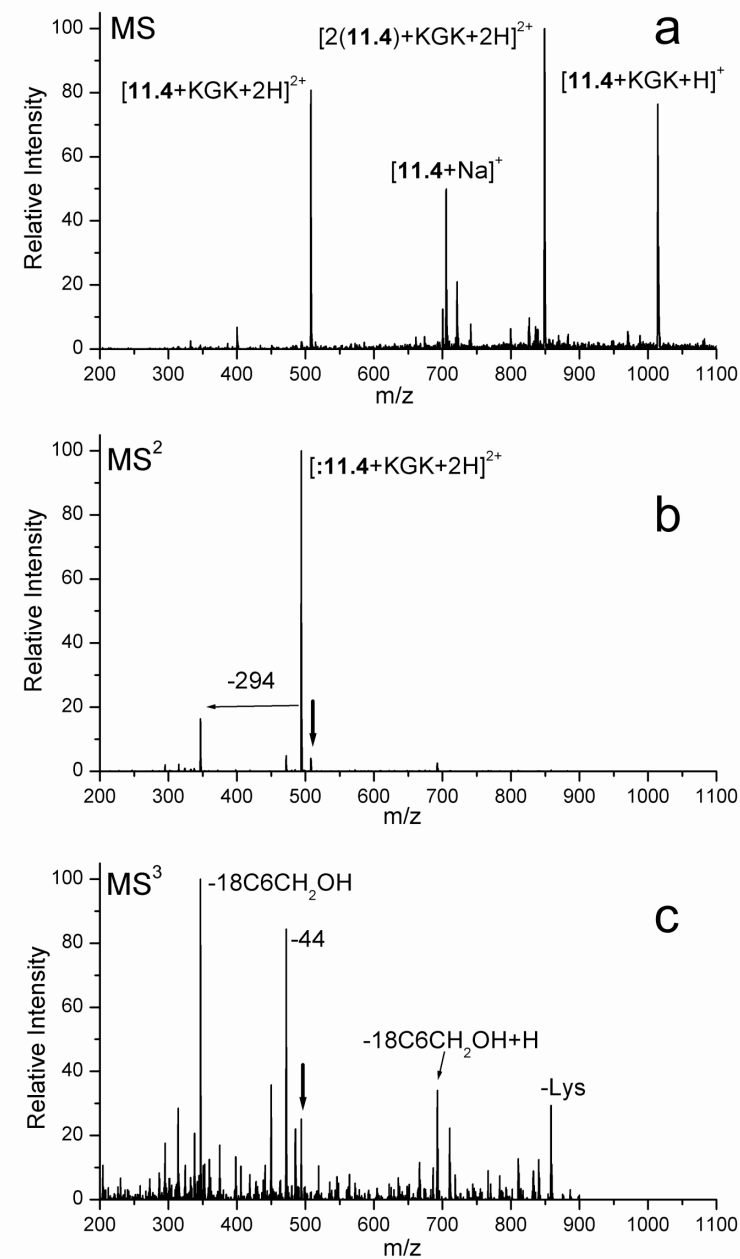


**Figure 11.6** (a) ESI-MS of KGK and **11.4** demonstrating abundant noncovalent complex formation. (b)  $MS^2$  on  $[11.4+KGK+2H]^{2+}$  yields the expected loss of  $N_2$ . (c) Further CAD reveals that the peptide has been trapped by the molecular mousetrap and the two molecules are now covalently attached. Bold downward arrows indicate peaks being subjected to CAD.

Reagent **11.5** only contains a single 18C6 and will therefore only bind to a single lysine, reducing the overall binding energy relative to **11.4**. The spectrum in Figure 11.7a shows that **11.5** forms abundant noncovalent complexes with KGK. Isolation and collisional activation of the doubly charged complex  $[\mathbf{11.5}+\text{KGK}+2\text{H}]^{2+}$  results exclusively in the loss of  $\text{N}_2$ , generating the reactive carbene in Figure 11.7b. Reisolation and further activation of this peak in Figure 11.7c yields fragments corresponding to the loss of the C-terminal and N-terminal lysine residues and the loss of 17 Da (presumably  $\text{NH}_3$ ). Simple dissociation is not observed, indicating covalent attachment through an intermolecular reaction occurred. The loss of lysine from both termini of the peptide suggests that either attachment of the crown is not selective for one lysine over another, or that the insertion reaction is not selective, or both.

CAD of the singly charged  $[\mathbf{11.5}+\text{KGK}+\text{H}]^+$  complex again results in loss of the neutral mousetrap **11.5** exclusively as seen in Figure 11.7d. The exact cause for this interesting behavior is not known, but the results can be explained by at least two possibilities. Either the binding energy of the complex is enhanced by the addition of a second proton, or the absence of the second proton enables a lower energy dissociation pathway. Regardless of the cause, it is observed in general that complexes with higher charge states tend to favor intermolecular reactions, while lower charge state complexes tend to favor simple dissociation. In very similar reactions to those shown in Figures 11.5b and 11.5c, reagent **11.5** has been covalently attached to many peptides including: INLKAI AALVKKVL, AAKRKAA, KPPGFSPFR, GGK, and GGKAA.

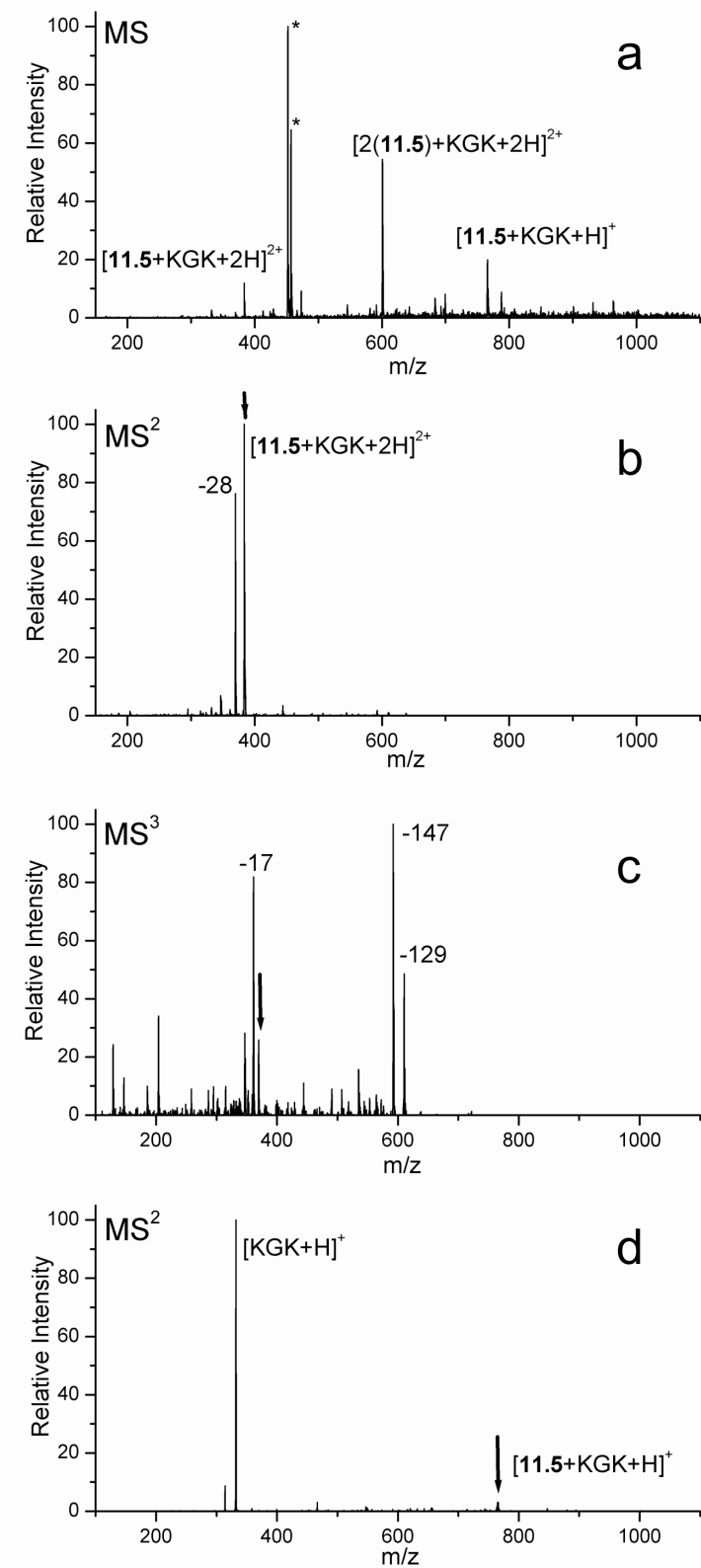


**Figure 11.7** Caption on next page.

**Figure 11.7** (a) ESI-MS of KGK and **11.5** demonstrating abundant noncovalent complex formation. (b)  $\text{MS}^2$  on  $[\mathbf{11.5}+\text{KGK}+2\text{H}]^{2+}$  yields the expected loss of  $\text{N}_2$ . (c) Further CAD reveals that the peptide has been trapped by the molecular mousetrap and the two molecules are now covalently attached. (d)  $\text{MS}^2$  on the singly charged complex results in simple dissociation. Bold arrows indicate peaks being subjected to CAD.

#### 11.4 Conclusion

These experiments demonstrate that development of biomimetic reagents capable of directing peptide chemistry in the gas phase is possible. The first successful examples of such reagents have been given. The search for a reagent that selectively cleaves peptides in the gas phase is still ongoing, but we have shown that with the proper combination of high binding energy and low reaction barriers, it is possible to initiate intermolecular reactions in noncovalent complexes with peptides. Furthermore, it is shown that sufficient binding energy to favor peptide cleavage over complex dissociation can be achieved with two 18C6 ethers attached to two lysines. Molecular mousetraps capable of covalently attaching to any lysine containing peptide are presented herein. This type of molecule represents the first step towards the development of gas phase cross-linking reagents. It is anticipated that the knowledge acquired from these initial results will allow for the development of other reagents capable of initiating controlled peptide chemistry in the gas phase. Although in the present study we have only considered the activation of these adducts to initiate covalent attachment in the gas phase, it should also be possible to effect similar chemistry in solution, with carbene formation initiated by either photochemical or metal catalyzed processes.<sup>20</sup>

## 11.5 References

---

<sup>1</sup> Vihinen, M. *Biomol. Eng.* **2001**, *18*, 241-248.

<sup>2</sup> (a) Tsaprailis, G.; Arpad, S.; Nikolaev, E. N.; Wysocki, V. H. *Int. J. Mass Spectrom.* **2000**, *195/196*, 467-479. (b) Tsaprailis, G.; Nair, H.; Somogyi, A.; Wysocki, V. H.; Zhong, W.; Futrell, J. H.; Summerfield, S. G.; Gaskell, S. J. *J. Am. Chem. Soc.* **1999**, *121*, 5142-5154.

<sup>3</sup> Lee, S. -W.; Kim, S. K.; Beauchamp, J. L. *J. Am. Chem. Soc.* **1998**, *120*, 3188-3195

<sup>4</sup> Lin, T.; Glish, G. L. *Anal. Chem.* **1998**, *70*, 5162-5165.

<sup>5</sup> Hu, P.; Loo, J. A. *J. Am. Chem. Soc.* **1995**, *117*, 11314-11319.

<sup>6</sup> Nemirovskiy, O. V.; Gross, M. L. *J. Am. Soc. Mass Spectrom.* **1998**, *9*, 1285-1292.

<sup>7</sup> Some reagents have been developed specifically for the gas phase: (a) Friess S.D.; Zenobi R. *J. Am. Soc. Mass Spectrom.* **2001**, *12*(7), 810. (b) Julian, R. R.; Akin, M.; May, J. A.; Stoltz, B. M.; Beauchamp, J. L. *Int. J. Mass Spectrom.* **2002**, *220*, 87-96.

<sup>8</sup> Julian, R. R.; Beauchamp, J. L. *Int. J. Mass. Spectrom.* **2001**, *210*, 613-623.

<sup>9</sup> For solution phase reagents, please see: (a) Bell, T. W.; Khasanov, A. B.; Drew, M. G. B.; Filikov, A.; James, T. L. *Angew. Chem. Int. Ed.* **1999**, *38*, 2543. (b) Galan, A.; Andreu, D.; Echavarren, A. M.; Prados, P.; de Mendoza, J. *J. Am. Chem. Soc.* **1992**, *114*, 1511. (c) Ludwig, R. Fresen. *J. Anal. Chem.* **2000**, *367*, 103. (d) Ngola S. M.; Kearney P. C.; Mecozzi S.; Russell K.; Dougherty D. A. *J. Am. Chem. Soc.* **1999**, *121*, 1192. (e) Rensing, S.; Arendt, A.; Springer, A.; Grawe, T.; Schrader, T. *J. Org. Chem.* **2001**, *66*, 5814, (f) Schrader, T. H. *Tetr. Lett.* **1998**, *39*, 517.

---

<sup>10</sup> (a) Schalley, C. A. *Mass Spectrom. Rev.* **2001**, *20*, 253-309. (b) Smith, R. D.; Bruce, J. E.; Wu Q. Y.; Lei, Q. P. *Chem. Soc. Rev.* **1997**, *26*, 191-202; (c) Veenstra, T. D. *Biophys. Chem.* **1999**, *79*, 63-79. (d) Loo, J. A. *Int. J. Mass Spectrom.* **2000**, *200*, 175-186.

<sup>11</sup> (a) Schwartz, B. L.; Light-Wahl, K. J.; Smith, R. D. *J. Am. Soc. Mass Spectrom.* **1994**, *5*, 201-204. (b) Nemirovskiy, O. V.; Ramanathan, R.; Gross, M. L. *J. Am. Soc. Mass Spectrom.* **1997**, *8*, 809-812. (c) Brodbelt, J. S. *Int. J. Mass Spectrom.* **2000**, *200*, 57-69. (d) Eckart, K.; Spiess, J. *J. Am. Soc. Mass Spectrom.* **1995**, *6*, 912-919.

<sup>12</sup> (a) Bradshaw, J. S.; Izatt, R. M.; Borkunov, A. V.; Zhu, C. Y.; Hathaway, J. K. *Comprehensive Supramolecular Chemistry*, Vol. 1; G. W. Gokel, Pergamon/Elsevier: Oxford, 1996; 35-95. (b) Maleknia, S.; Brodbelt, J. *J. Am. Chem. Soc.* **1993**, *115*, 2837-2843.

<sup>13</sup> Julian, R. R.; Beauchamp, J. L. *J. Am. Soc. Mass Spectrom.* **2002**, *13*, 493-498.

<sup>14</sup> Julian, R. R.; May, J. A.; Stoltz, B. M.; Beauchamp, J. L. *Angew. Chem. Int. Ed.* **2003**, *42*(9), 1012-1015.

<sup>15</sup> a) Chandler, C. J.; Deady, L. W.; Reiss, J. A. *J. Heterocyclic Chem.* **1981**, *18*, 599. b) Weijnen, J. G. J.; Koudijs, A.; Schellekens, G. A.; Engbersen, J. F. *J. J. Chem Soc. Perkin Trans. 2* **1992**, 830.

<sup>16</sup> Steen, H.; Jensen, O. N. *Mass Spectrom. Rev.* **2002**, *21*, 163-182.

<sup>17</sup> The insertion reaction only occurs when the H-C-H bond is presented symmetrically to the carbene, suggesting a minimal barrier may exist. Higher level DFT calculations at the at the B3LYP/CCPVTZ(-F)<sup>+</sup> level on :11.6 yield a singlet ground state with a singlet/triplet splitting of 3±1 kcal/mol suggesting that these reactions may proceed through the singlet state.

---

<sup>18</sup> Toscano, J. P.; Platz, M. S.; Nikolaev, V.; Popic, V. *J. Am. Chem. Soc.* **1994**, *116*, 8146-8151.

<sup>19</sup> Moss, R. A.; Jones, M., Jr. Eds. *Carbenes, Vols. 1 and 2*; Wiley: New York, 1973, 1975.

<sup>20</sup> (a) Doyle, M. P.; McKervey, M. A.; Ye, T. *Modern Catalytic Methods for Organic Synthesis with Diazo Compounds*; Wiley-Interscience: New York, 1998. (b) Moody, C. J.; Whitham, G. H. *Reactive Intermediates*; Oxford University Press: New York, 1992; 26-50.